

ORIGINAL ARTICLE

MIF-CD74 signaling impedes microglial M1 polarization and facilitates brain tumorigenesis

A Ghoochani^{1,5}, MA Schwarz^{1,5}, E Yakubov¹, T Engelhorn², A Doerfler², M Buchfelder¹, R Bucala³, NE Savaskan^{1,4,6} and IY Eyüpoglu^{1,6}

Microglial cells in the brain tumor microenvironment are associated with enhanced glioma malignancy. They persist in an immunosuppressive M2 state at the peritumoral site and promote the growth of gliomas. Here, we investigated the underlying factors contributing to the abolished immune surveillance. We show that brain tumors escape pro-inflammatory M1 conversion of microglia via CD74 activation through the secretion of the cytokine macrophage migration inhibitory factor (MIF), which results in a M2 shift of microglial cells. Interruption of this glioma–microglial interaction through an antibody-neutralizing approach or small interfering RNA (siRNA)-mediated inhibition prolongs survival time in glioma-implanted mice by reinstating the microglial pro-inflammatory M1 function. We show that MIF-CD74 signaling inhibits interferon (IFN)- γ secretion in microglia through phosphorylation of microglial ERK1/2 (extracellular signal-regulated protein kinases 1 and 2). The inhibition of MIF signaling or its receptor CD74 promotes IFN- γ release and amplifies tumor death either through pharmacological inhibition or through siRNA-mediated knockdown. The reinstated IFN- γ secretion leads both to direct inhibition of glioma growth as well as inducing a M2 to M1 shift in glioma-associated microglia. Our data reveal that interference with the MIF signaling pathway represents a viable therapeutic option for the restoration of IFN- γ -driven immune surveillance.

Oncogene (2016) 35, 6246–6261; doi:10.1038/onc.2016.160; published online 9 May 2016

INTRODUCTION

With a median survival time of ~1 year, primary malignant brain tumors belong to one of the most threatening tumor entities.¹ The poor prognosis is attributed to the ability to induce angiogenesis,² uncontrolled tumor proliferation and invasion³ of surrounding brain parenchyma. A further hallmark of this tumor entity lies in the ability to modify the tumor microenvironment with induction of perifocal edema,⁴ with a resultant, drastic increase in mass effect. Manifesting as cerebral edema, it mandates prior management due to typically rapid neurological deterioration before definitive surgery.⁵ This process entails the release of neurotoxic factors,^{6,7} which in turn intervene in the modulation of the neuro-immune system.^{8,9} Resident microglial cells are in an extraordinary position to protect the central nervous system through antigen presentation and phagocytosis in an immune-privileged area. Their lack can therefore lead to massive neuronal damage.^{10,11}

Any disturbance in neuronal homeostasis leads to the accumulation and activation of microglia,^{10,12} the role of which in tumor proliferation and surveillance and the mechanisms of tumor escape is little known.⁸ What is confirmed is that microglial cells show an increased accumulation in peritumoral tissue as well as diffuse infiltration into the tumor mass without eliciting immunological or phagocytic responses.^{8,13} Further, glioma-modulated microglial cells in the brain tumor microenvironment enhance tumor malignancy and are associated with poor prognosis.^{14,15} This indicates the presence of an immune-suppressive tumor microenvironment shifting microglia to an

immune-paralyzing and tumor-promoting M2 phenotype.¹⁵ Immune-modulating cytokines secreted by malignant gliomas have been identified, notably colony stimulating factor 1 (CSF-1), glial derived neutrophic factor (GDNF) and transforming growth factor beta (TGF- β), which contribute to the development of an immunosuppressive environment.^{16–19} In this manner, immune ‘escape mechanisms’ have a decisive role in tumor infiltration and proliferation.

Although the biological function of microglia is yet to be unequivocally defined in neuro-oncology, tumor inhibition through the modulation of microglial inhibition is possible at least in experimental settings. As derived microglia are generally capable of phagocytosis and accumulate in the tumor bed, this cell population could be instrumental in the treatment of malignant gliomas. A reprogramming of these cells with cancellation of the tumor-induced paralysis, combined with the ability to cross the blood–brain barrier, would predestine microglia for a neuro-immunological attack on tumor cells. The cytokine macrophage migration inhibitory factor (MIF) is an upstream regulator of innate immunity and a potent cancer growth regulator and may therefore have an essential role in this context.^{20,21} MIF signals upstream of cytokines—such as tumor necrosis factor (TNF)- α , interferon (IFN)- γ and interleukin (IL)-1 β via receptor binding in CD74-dependent pathways^{22,23} as well as being associated with the promotion of neoplastic cell proliferation and survival of a different origin involving the ERK1/2-MAPK pathway.^{21,24} Additionally, despite any autocrine effects, MIF also transmits signals to the brain parenchyma and in particular to microglial cells.

¹Department of Neurosurgery, Universitätsklinikum Erlangen, Medical Faculty of the Friedrich Alexander University of Erlangen-Nürnberg (FAU), Erlangen, Germany; ²Department of Neuroradiology, Universitätsklinikum Erlangen, Medical Faculty of the Friedrich Alexander University of Erlangen-Nürnberg (FAU), Erlangen, Germany; ³Department of Internal Medicine, Yale University School of Medicine, New Haven, CT, USA and ⁴BiMECON Ent., Kurfürstenstrasse 21, Berlin, Germany. Correspondence: Dr IY Eyüpoglu, Department of Neurosurgery, Universitätsklinikum Erlangen, Medical Faculty of the Friedrich Alexander University of Erlangen-Nürnberg (FAU), Schwabachanlage 6, 91054 Erlangen, Bayern, Germany. E-Mail: ilker.eyupoglu@uk-erlangen.de or eyupoglu@gmx.net

⁵These authors contributed equally to this work.

⁶These authors contributed equally as senior authors.

Received 1 September 2015; revised 17 December 2015; accepted 23 February 2016; published online 9 May 2016

RESULTS

MIF knockdown in malignant gliomas promotes microglial attack
 To identify glioma-derived cytokines involved in immune surveillance mechanisms, we analyzed cytokine expression levels in malignant gliomas by using the ONCOMINE data-mining platform. It was clearly seen that the expression of MIF was significantly

higher in glioblastoma patients (WHO[°]IV) as opposed to the control group. (Figure 1a).²⁵ This correlates with our own analyses of MIF expression in WHO[°]I–[°]IV gliomas. WHO[°]IV gliomas (GBM) have significantly increased MIF expression compared with controls (Figure 1b). Malignant glioma cell lines U87MG (human), F98 (rat), GL261 (mouse) as well as primary glioblastoma tissue

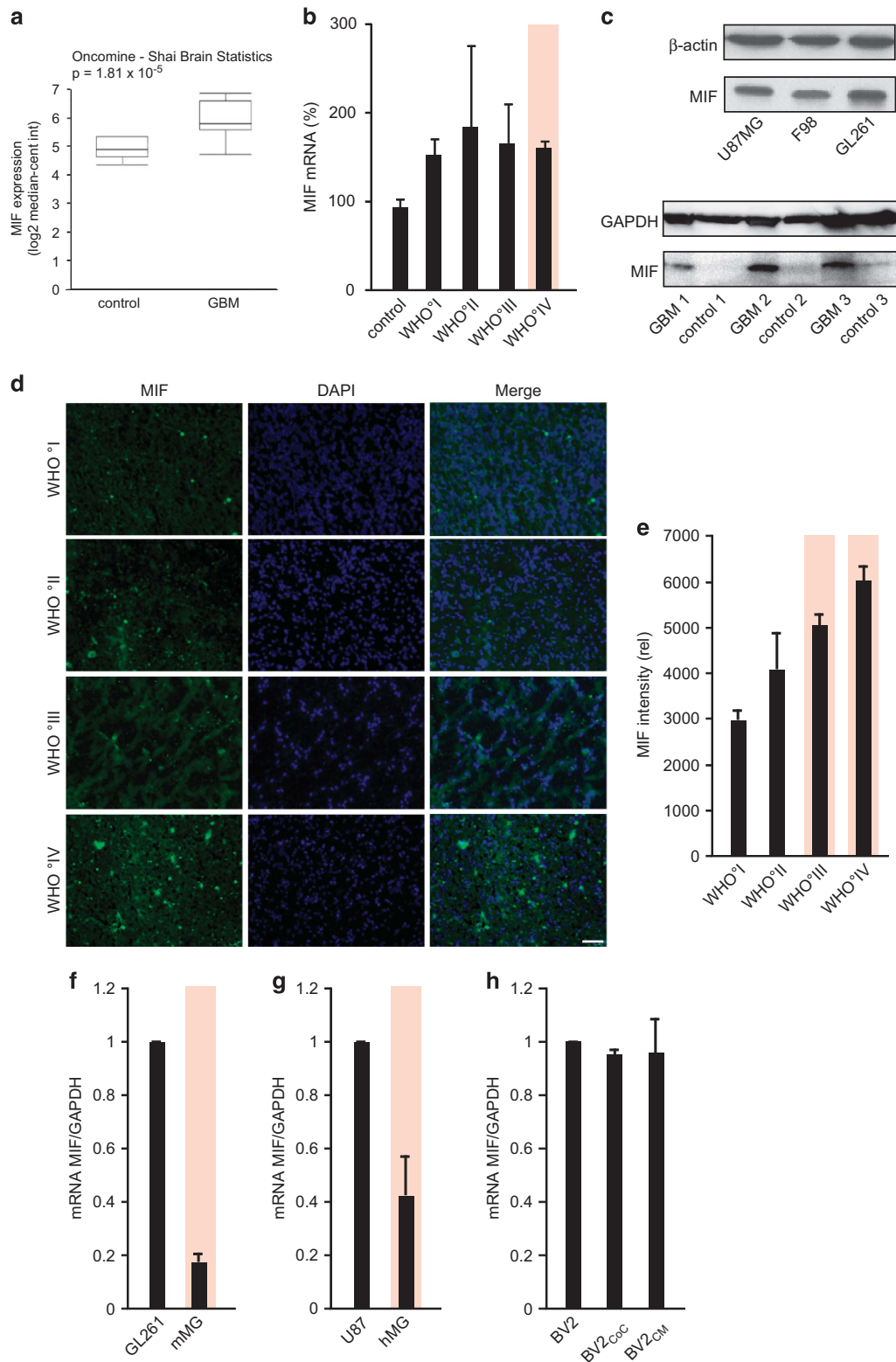


Figure 1. For caption see page 6248

from three typical patients displayed a prominent overexpression of the MIF protein compared with normal brain parenchyma (Figure 1c), confirmed by MIF-specific immunofluorescence analysis: the higher the WHO°, the more intensive the MIF expression (Figures 1d and e). A correlative expression analysis conducted to differentiate between increased MIF secretion attributed to microglia or to glioma cells showed a significantly higher MIF expression in malignant gliomas (Figures 1f and g). Even treatment with conditioned medium failed to stimulate MIF secretion in microglia (Figure 1h).

In order to elucidate the extent to which MIF expression is critical to glioma survival, we pharmacologically suppressed MIF activity in F98 glioma cells through the MIF-specific inhibitor ISO-1.²⁶ There was no significant difference compared with untreated controls with regard to cell survival (Figures 2a and b). We next generated MIF-silenced U87MG and F98 glioma cells through three specific small interfering RNAs (siRNAs; Figure 2c). In addition, we created U87MG and F98 glioma cells with overexpression of the cytokine MIF (Figure 2d). The MIF secretion was subsequently analyzed by enzyme-linked immunosorbent assay (ELISA) showing significantly elevated MIF secretion in MIF-overexpressing glioma cells (pMIF) and a successful suppression of MIF secretion using two independent siRNAs (siMIF #1 and #2; Figure 2e). The introduction of siRNA-mediated inhibition of MIF expression in U87MG and F98 glioma cell lines caused neither any morphological change (data not shown) nor any significant change in cell proliferation (Figure 2f). To understand the role of MIF *in vivo* we implanted control gliomas and MIF knockdown tumors into mouse brains with subsequent monitoring of tumor growth by live animal imaging. For that we chose magnetic resonance imaging (MRI) scans at an early time point before the occurrence of clinical symptoms. Analysis of the glioma-implanted mice (Figure 2g) showed a significantly reduced tumor volume in the group with MIF-deficient gliomas (Figure 2h), whereas no significant difference in proliferation could be identified *in vitro* (Figure 2f). Correspondingly, the mice in the group with MIF-deficient gliomas survived significantly longer than animals with MIF-secreting wild-type gliomas (Figure 2i).

Immunohistochemical analysis showed an altered accumulation of microglia in the group with inhibited MIF expression of glioma cells (Figures 3a and b). Normally, a conspicuous accumulation of microglia is found in peritumoral tissue, whereas only a low number of microglial cells are visible within the tumor itself (Figure 3a). In contrast, MIF-silenced gliomas showed significant increase of microglial infiltration (Figure 3b), implying that the siRNA-mediated inhibition of MIF neutralizes the ‘paralysis’ of microglia in malignant gliomas. One possible MIF signaling pathway involves CD74 receptor-dependent mechanisms in immune cells.^{23,27} We studied the expression of the MIF receptor CD74 in primary human glioma specimens in order to determine the clinical relevance of this signaling pathway. Normal human brain tissue specimens (control—white matter) showed random

distribution of microglial cells (Figure 3c). Human brain tissue with diagnosed glioblastoma (WHO°IV), however, showed microglial accumulation at the tumor border as visualized by IB4 staining, whereas the tumor core was devoid of microglial cells (Figure 3c). Importantly, CD74 expression was identified in peritumoral tissue and co-localized with microglia cells (Figure 3c). To investigate the underlying mechanisms of MIF-induced microglial paralysis, we first analyzed the expression of CD74 receptor messenger RNA in primary murine (mMG), in primary human microglia (hMG) and in microglia cell line (Figure 3d). We then silenced the MIF receptor CD74 on microglial cells through RNA interference (Figure 3e). Although proliferation and overall microglial morphology were not affected (Figure 3f), elevated migratory activity monitored in Boyden chamber assay was observed after suppression of the CD74 receptor (Figure 3g).

As MIF acts in long distance, we treated microglial cells with conditioned media from gliomas in the next set of experiments (Figure 4a). Although microglia treated with MIF-reduced supernatant showed no alteration on proliferation, treatment of wild-type microglia with MIF-enriched supernatant significantly reduced proliferation activity (Figure 4a). Accordingly, treatment of CD74-silenced microglia with MIF-enriched supernatant cancels this proliferation effect, indicating the relevance of CD74 receptor for MIF signaling (Figure 4a). To test their cellular potency we next co-cultured either wild-type microglial cells or CD74-silenced microglia cells with glioma cells (Figure 4b). Five days after co-culturing, CD74 knocked down microglia entangled and significantly reduced the number of glioma cells (Figure 4c), indicating that CD74 knocked down microglia attack malignant gliomas independent of their MIF phenotype (Figure 4b). Co-implantation of wild-type microglia and glioma cells into brain tissue revealed unrestricted glioma growth and reduced microglial migration in an *in vivo*-like environment (Figures 4d and e). However, microglia with disrupted CD74 receptor complex showed a rapid migratory activity toward the site of the tumor (Figure 4e) and blocked its growth (Figure 4f). To unequivocally prove that glioma-derived MIF secretion impacts microglial activity and tumor progression, we tested CD74 knockdown microglia *in vivo*. We orthotopically implanted syngeneic glioma cells into mouse brains and co-implanted microglial cells following stable *in vivo* tumor growth. To confirm the blocked immune escape mechanisms of malignant gliomas, we performed histological analysis of tumor-implanted brains (Figure 4g). We found significant higher numbers of microglial cells surrounding the tumor (Figure 4h). Moreover, brain tumors were infiltrated by CD74-silenced microglia whereas tumors with wild-type microglia respected the brain–tumor border and hardly showed any tumor infiltration (Figure 4g), confirming our data found in MIF knockdown gliomas (Figures 3a and b). Accordingly, mice with CD74-silenced microglia showed prolonged survival in comparison to tumor-bearing mice with wild-type microglial cells (Figure 4i).

Figure 1. Increased MIF expression by human malignant gliomas. **(a)** Analysis of MIF expression by ONCOMINE data-mining platform.²⁵ MIF was significantly higher in glioblastoma patients (WHO°IV, $n = 27$) as opposed to the control group ($n = 7$; $P = 0.0000181$). **(b)** MIF expression was analyzed by quantitative reverse transcriptase (RT)–PCR in different astrocytomas. Each group contains at least three samples. MIF was significantly higher expressed in glioblastoma patients (WHO°IV) compared with control (con). **(c)** 1st panel, expression of the cytokine MIF in human (U87), rodent (F98) and murine (GL261) glioma cell lines; β -actin serves as a loading control. 2nd panel, MIF immunoblots from representative human glioblastoma samples (GBM 1, 2 and 3) and human brain samples without malignant tumors (control 1, 2 and 3). Immunoblotting for GAPDH serves as a loading control. **(d)** Human tissue sections of different astrocytoma grades were analyzed for MIF expression by immunofluorescence. Each group contained at least three samples. The panels show MIF staining (MIF—green) and nuclei staining (4',6-diamidino-2-phenylindole (DAPI)—blue). Right panel gives merged images of each row. Scale bar, 50 μ m. **(e)** Quantitative analysis by immune staining showed MIF expression to be directly proportional to WHO°, with a correspondingly significantly high expression of MIF in WHO°III and °IV gliomas. **(f)** Quantitative RT–PCR analysis shows significantly higher MIF expression in murine glioma cells (GL261) in comparison to primary murine microglia (mMG). **(g)** Quantitative RT–PCR analysis shows significantly higher MIF expression in human glioma cells (U87) in comparison to primary human microglia (hMG). **(h)** Additional quantitative RT–PCR analysis of MIF expression in the BV2 microglia cell line shows no increase in MIF secretion following co-culture with glioma cells (BV2_{coC}) or following treatment with conditioned glioma medium (BV2_{CM}).

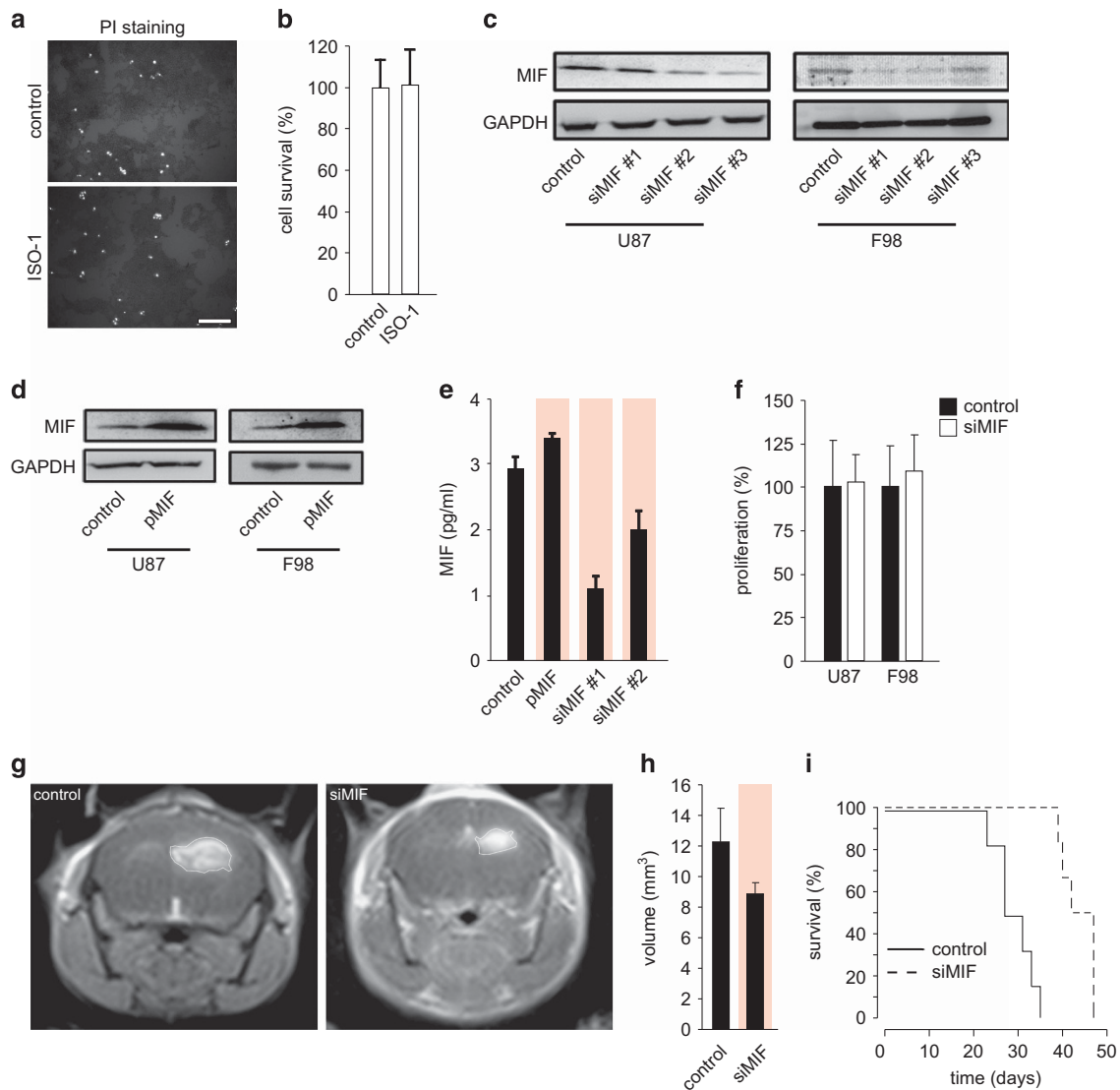


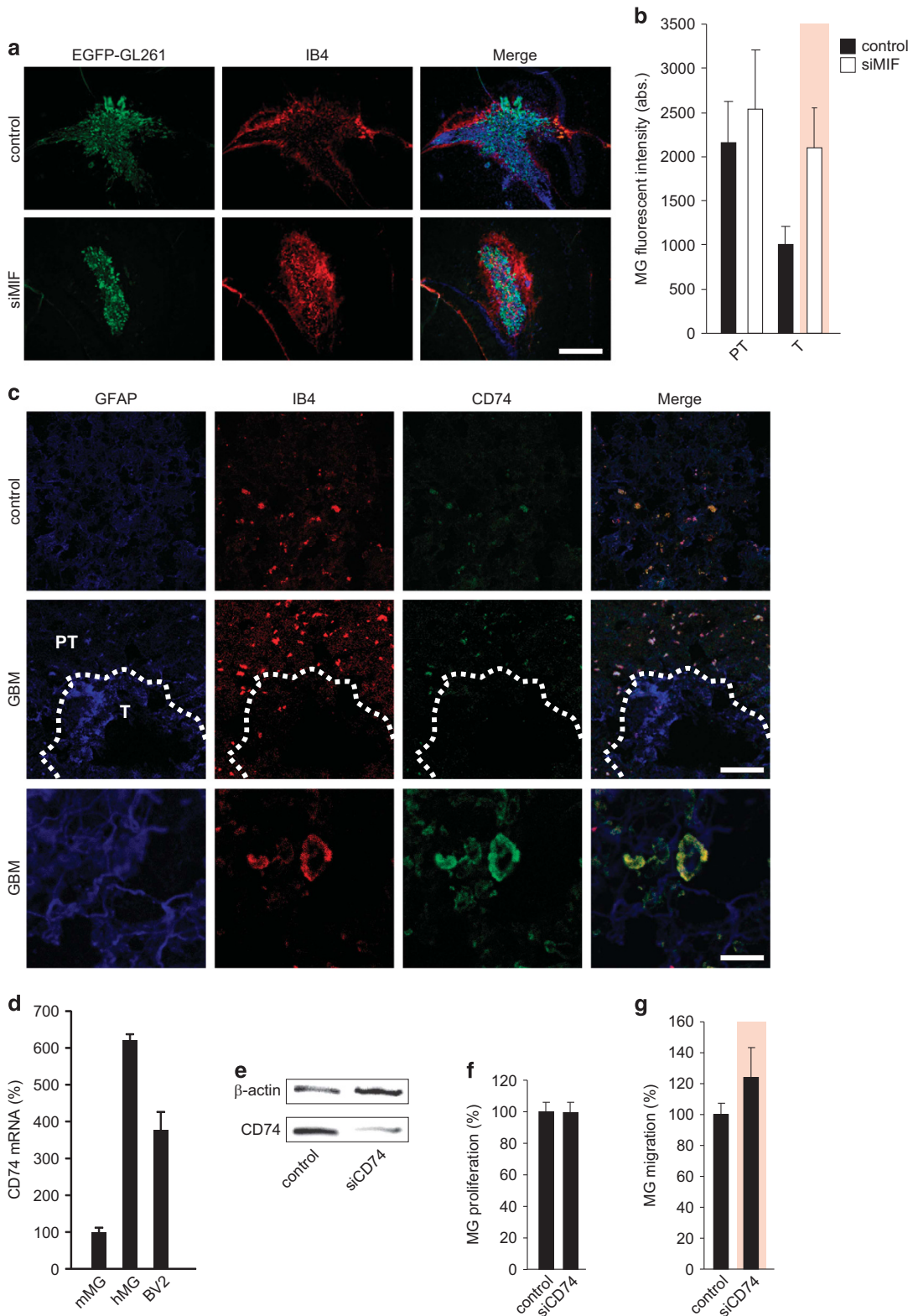
Figure 2. MIF suppression in gliomas silences tumor progression *in vivo*. **(a)** Treatment of F98 glioma cells with 100 μM of the MIF inhibitor ISO-1 for 72 h does not increase cell death, which was visualized by propidium iodide (PI) staining. Scale bar, 30 μm . **(b)** *In vitro* F98 glioma cell survival analysis using 3-(4,5-dimethylthiazol-2-yl)-2,5-diphenyltetrazolium bromide (MTT) assay, control compared with 100 μM ISO-1 treatment. The assay was independently repeated three times with $n = 12$. **(c)** siRNA-mediated MIF knockdown (siMIF#1, #2 and #3) in human (U87) and rodent (F98) glioma cells, as revealed by immunoblotting. Controls are transfected with scrambled siRNAs; GAPDH serves as an internal loading control. **(d)** Overexpression of MIF (pMIF) in human (U87) and rat (F98) glioma cells. GAPDH serves as an internal loading control. **(e)** MIF secretion was analyzed by ELISA from F98 glioma supernatants ($n = 3$). A significantly elevated MIF secretion was identified for pMIF, whereas a significantly reduced MIF secretion resulted in siMIF#1 and siMIF#2. **(f)** *In vitro* proliferation analysis of wild-type gliomas (human (U87) and rodent (F98); black columns) and gliomas with silenced MIF expression (white columns). The proliferation assay was repeated three times with $n = 12$. **(g)** Representative MRI analysis of wild-type gliomas and MIF knockdown gliomas (siMIF) 10 days after tumor implantation. The tumor bulk (dotted line) was visualized by intraperitoneally applied contrast agent before T1-weighted imaging. **(h)** Quantification of T1-weighted MR images of six animals each group (wild-type gliomas vs siMIF gliomas). **(i)** Kaplan–Meier survival curves of mice implanted with control gliomas (wild type, $n = 6$) or MIF knockdown gliomas (siMIF, $n = 6$).

Besides the siRNA-mediated silencing of the CD74 receptor, this receptor could also be inhibited by monoclonal antibody blocking approach (Figure 5a). Noteworthy, direct exposure to the monoclonal antibody had no effect on glioma cell viability (Figure 5b), confirming that the hitherto observed inhibition of glioma growth cannot be solely attributed to the direct interaction between secreted MIF and CD74 receptors alone. However, treatment of the tumor with CD74-specific monoclonal antibodies in an organotypic environment (Figures 5c–f) led to a significant deceleration in tumor growth through massive tumor infiltration by microglial cells (Figures 5c–f). Likewise, we found the same

effects on gliomas in the case of the siRNA-mediated silencing of CD74 *in vivo* (Figures 4f and g). These data support the concept that malignant gliomas secrete MIF to activate microglial CD74 receptors, inducing microglial paralysis. In order to assess the influence of inert microglia, we utilized transgenic mice, which express GFP under the microglia-specific promoter CX3CR1. After implantation of red fluorescing GL261 glioma cells, we treated brain slice cultures of these mice with either a monoclonal antibody against CD74 or recombinant MIF (Figure 5g). Treatment of living organotypic brain slice cultures with the CD74 antibody induced microglial infiltration of the tumor as observed in the case of exogenous implanted microglia

(Figures 5g and h). Treatment with recombinant MIF leads to a corresponding inhibition of this effect so that the microglia once again displayed respect for the tumor borders as observed in controls (Figures 5g and h).

MIF-CD74 signaling impedes M2 into M1 polarization of glioma-associated microglia
 As MIF-CD74 signaling pathway modulates two relevant characteristics of microglia, that is, phagocytotic activity and cytotoxic



potency, the question at the heart of the debate is to what extent this pathway is also associated with the M1/M2 polarization of glioma-associated microglial cells. In other words: is the MIF-dependent modulation of phagocytosis and cytotoxicity of microglial cells a characteristic that attributes to their M1/M2 polarization. We therefore analyzed the ability of MIF to induce a microglial polarization toward M2 or M1. We first tested F98 glioma cells, which were genetically modified by their MIF secretion (expressing pMIF or a siMIF gene construct) and co-cultured these cells with primary rat microglia. M1 parameters were thereafter measured by quantitative RT-PCR. Although glioma cells with elevated MIF secretion hindered microglial shifting to the glioma harming M1 phenotype, silencing of glioma MIF secretion enabled a significant upregulation of M1 parameter expression (Figure 6a). In contrast, sole MIF expression did not suppress M1 marker expression (Figure 6a). In the next set of experiments we treated primary murine microglial cells with recombinant MIF and analyzed subsequently the expression of M2 markers (Figure 6b). After MIF treatment we observed a significant shift toward the M2 phenotype with increased expression of CD204, TGF- β , IL-10 and Arg-1 (Figure 6b). We further tested F98 glioma cells, which were genetically modified by their MIF secretion and co-cultured these cells with primary rat microglia. Increased MIF secretion (pMIF) in F98 glioma cells clearly correlated with elevated M2 marker expression in primary rat microglia (Figure 6c). Conversely, microglia treated with conditioned media from MIF-silenced gliomas did not shift toward a M2 status. Moreover, CD74 inhibition by monoclonal antibody treatment (CD74_{mAb}) diminished MIF-induced M2 transformation in MIF-expressing co-cultures (Figure 6c). This microglial shift was also observed in an *in vivo* experiment (Figure 6d). We implanted GL261 glioma cells into mouse brain and analyzed expression of the M1 and M2 markers CD86 and Arg-1. CD86 as a representative marker for M1 polarization was significantly increased in MIF-silenced gliomas compared with wild-type MIF-expressing glioma cells (Figure 6e). Arg-1 as a representative marker for M2 polarization was conversely decreased in MIF-silenced gliomas compared with wild-type MIF-expressing gliomas (Figure 6e). These data show that MIF modulates microglial cells toward a M2 activation status in a CD74-dependent manner.

We performed both phagocytosis and cytotoxicity assays in order to examine the effect of microglial infiltration on glioma cells. Treatment of murine microglia with recombinant MIF significantly diminished their phagocytotic activity with reduced identification of intracellular latex beads in microglial cells (Figures 7a and b). In order to define the extent of microglial cytotoxicity on glioma growth, we co-cultivated microglial cells with GL261 glioma cells and treated these cultures with recombinant MIF in the presence or absence of CD74-blocking antibodies. After co-culturing tumor cells with microglia, GL261 glioma cells were analyzed for cell death by fluorescence

activated cell sorting (FACS) analysis (Figure 7c). Treatment with recombinant MIF significantly reduced microglial toxicity on glioma cells and this effect could be reversed by combined treatment together with CD74 (Figure 7d). Further analysis of polarization status (Figures 7e and f) in order to test our hypothesis attributing the retarded phagocytosis and cytotoxicity to a biased M1/M2 polarization of MIF treated microglia (Figure 7a) showed a pronounced shift toward M2 polarization (Figures 7e and f).

Microglial IFN- γ secretion reinstates into M1 polarization via an autocrine loop

As CD74 knockdown microglia revealed long-range tumor inhibitory activity, we hypothesized that secretory factors—such as an inflammatory cytokines—could be responsible for this response. To this effect, we investigated the cytokine profile of CD74 knockdown microglia with cytokines secreted from wild-type microglia. Whereas most analyzed cytokines such as IL-1, IL-2 and IL-4 were characterized by equal secretion levels in both supernatants, IFN- γ was significantly elevated in CD74-silenced microglial cells (Figure 8a).

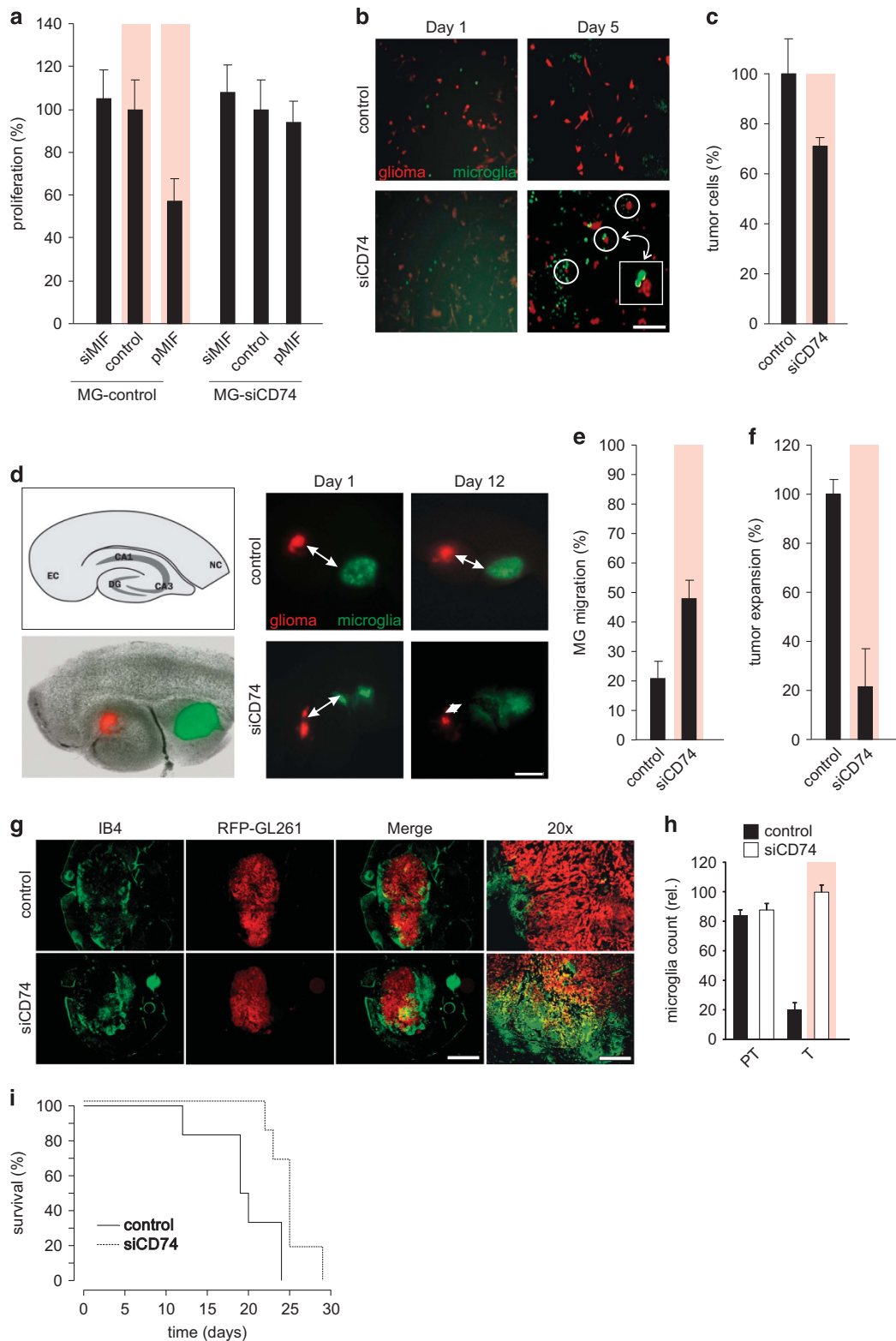
To confirm that MIF-CD74 signaling includes involvement of IFN- γ activity and merges in a common pathway, we treated primary murine microglia with MIF and analyzed the corresponding IFN- γ expression by quantitative RT-PCR. Noteworthy, MIF treatment abolished microglial IFN- γ expression (Figure 8b). Further, we tested whether MIF-induced ERK signaling is involved in IFN- γ release. For this, we treated microglial cells with the ERK inhibitor PD98059 or with the MEK inhibitor U0126 in the presence of recombinant MIF. These blocking experiments revealed that MIF-induced IFN- γ suppression could be reversed by ERK1/2 inhibition (Figure 8b).

As MIF-CD74 signaling utilizes ERK1/2 activation to execute its downstream effects, we tested this in glioma-associated microglial cells. For this we treated microglial cells with conditioned media from gliomas and analyzed the ERK1/2 activation. Supernatants from wild-type gliomas and MIF-overexpressing gliomas induced ERK1/2 phosphorylation in microglial cells (Figure 8c). Hence, knocking down CD74 in microglial cells blocked MIF-induced ERK1/2 activation. Furthermore, phosphorylation of ERK1/2 was diminished following treatment of microglia with supernatants from MIF-overexpressing gliomas (Figure 8c). Thus, CD74-silenced microglia did not show ERK1/2 activation upon glioma-conditioned media or recombinant MIF treatment, indicating that MIF executes its signaling effects on microglia through CD74-dependent signaling.²⁸ Treating microglial cells with recombinant MIF correspondingly resulted in an increased phosphorylation of ERK1/2. Moreover, treatment with the ERK1/2 inhibitor PD98059 or with the MEK inhibitor U0126 diminished MIF-induced ERK1/2 phosphorylation in microglial cells (Figure 8c). These data indicate that MIF-CD74 signaling executes its effects via downstream activation of the ERK pathway. Altogether, these data confirm

Figure 3. Glioma derived MIF activates microglial CD74. **(a)** Brains of wild-type glioma implanted (control) and MIF knockdown implanted gliomas (siMIF) were cryo-sectioned and analyzed for glioma growth and microglia infiltration. Upper row shows wild-type glioma expansion (green), microglial distribution (red) and nuclei staining (blue). Lower panel shows microglial distribution in gliomas with siRNA-silenced MIF. Scale bar, 3 mm. **(b)** Quantification of microglial cells in peritumoral region (PT), and tumor bulk (T) in wild-type gliomas (black columns) and MIF knocked down gliomas (white columns) with $n = 4$. **(c)** Human brain tissues were cryo-sectioned and analyzed for microglial distribution. Human microglial cells are accumulated in peritumoral regions and CD74+ in glioblastoma affected brain tissue. Upper panel shows representative image of astroglial distribution (blue, GFAP), microglial cells (red, IB4) and CD74 expression (green) in human brain tissue (non-malignant brain tissue, control). Right panel gives merged images of each row. Microglial cells (red, IB4+) are accumulated in peritumoral regions and co-localized with CD74 (green) in human brains diagnosed for glioblastoma (GBM, revealed by GFAP immunostaining, blue). Lower panel, higher magnification of CD74 (green) positive microglial cells (IB4, red). Scale bar in middle column represents 70 μ m and in lower column 5 μ m. **(d)** Expression of CD74 in primary murine, human and BV2 microglia was analyzed by quantitative RT-PCR. **(e)** Expression of CD74 in BV2 microglial cells (control) and BV2 microglial cells with siRNA-mediated CD74 knockdown (siCD74) revealed by representative immunoblotting. β -Actin serves as a loading control. **(f)** Microglial proliferation is not affected, **(g)** whereas siRNA-mediated CD74 silencing in microglial cells alleviates migration. The experiments were repeated three times with $n = 12$.

that glioma-associated MIF secretion induces elevated ERK phosphorylation in microglia leading to a suppression of IFN- γ expression. During the course of further investigations of the possible effects of IFN- γ on tumors, we treated F98 and GL261 glioma cells with IFN- γ and subsequently analyzed proliferation

activity. We found that IFN- γ impairs glioma proliferation in a concentration-dependent manner with significant effect already at 1 pg/ml (Figure 8d). We further used the *ex vivo* organotypic glioma invasion model (OGIM) with implantation of glioma cells alone and investigated the impact of an enriched IFN- γ



environment on tumor progression (Figure 8e). In controls, glioma cells grew over time and infiltrated normal brain tissue (Figure 8f). In the case of enriched IFN- γ levels, tumor progression was slowed down in a concentration-dependent manner (Figure 8f), indicating that MIF-induced CD74 signaling affects downstream IFN- γ expression.

We could show that IFN- γ suppresses glioma growth directly. Next, we tested whether IFN- γ has an impact on microglial polarization. For this, we treated primary murine microglia with IFN- γ and processed the M1 parameters, that is, IL-1 β , CD11b, CD86 and TNF α . Almost all M1 parameters, excluding CD11b, were significantly elevated, indicating that IFN- γ is a potent cytokine executing a M1-polarized microglial status (Figure 8g). Short hairpin-mediated silencing of IFN- γ receptor significantly decreases M1 polarization (CD86 as a representative M1 marker) compared with control microglia (Figures 8h and i). We further co-cultured MIF-silenced glioma cells either with wild-type microglia or IFN- γ receptor silenced microglia and analyzed the microglial ability to induce glioma cell death (Figure 8j). Microglial cells kill MIF-silenced glioma cells, as expected (Figure 8k). This effect was completely abolished when the microglial IFN- γ receptor was silenced (Figure 8k), finally confirming that glioma MIF signaling acts via IFN- γ receptor axis (Figure 9).

DISCUSSION

Despite current therapeutic approaches including surgery, chemotherapy and radiotherapy high-grade gliomas including glioblastomas have still deadly prognosis.^{1,29} Malignant tumor cells modify their microenvironment to optimize their own progression thus forming an alternative strategy to target gliomas.^{30,31} In order to better understand microglia tumor microenvironment and interaction, we analyzed the expression of candidate molecules secreted by malignant gliomas. Here, we identified the cytokine MIF which is expressed and secreted by malignant gliomas. The MIF expression in malignant gliomas exceeds by far the levels found in normal brain tissue. Noteworthy is the fact that increased MIF expression is clinically associated with a worse prognosis and earlier tumor recurrence in malignant gliomas.^{1,32,33} To test the relevance of MIF in the tumor microenvironment we introduced specific modifications in the MIF signaling pathway. Interestingly, genetic and pharmacological MIF inhibition in malignant gliomas did not cause any morphological changes nor altered significantly cell proliferation independent of residual or bone marrow-derived microglial cells. However, tumor implantation *in vivo* revealed that animals with MIF-deficient tumors lived significantly longer than the control groups, correlating with a significantly smaller tumor volume in MR imaging studies. Immunohistochemical analysis showed an

altered accumulation of microglia in the glioma group with inhibited MIF expression. We further blocked the glioma MIF axis by inhibition MIF receptor activation. The trans-membrane CD74 receptor (DHLA/HLA class II histocompatibility antigen gamma chain) and its co-receptor CD44 (CSPG8/MIC4) are MIF receptors transmitting macrophage/microglial migration inhibition and proliferative effects through ERK1/2 downstream activation.^{23,27} Alternative MIF receptors have been described with the CXC chemokine receptors CXCR2 and CXCR4 having a relevant role especially in inflammatory processes.^{20,34} The activation of these receptors during inflammation leads to the recruitment of T cells and monocytes. However, resident microglial cells express mainly CD74 compared with CXCR2 and CXCR4 thus indicating a prominent role for MIF signaling in the brain.^{35,36} This is also the reason why we did not further differentiated the analysis on bone marrow-derived myeloid cells and T cells. In addition, over 80% of tumor-associated microglia are resident microglia originating from the brain itself.³⁷ Only in late course of the disease myeloid cells will follow microglial cell accumulation.³⁷ As our analysis focused on the progress of the disease in early stages, we used assays which allowed to specifically investigate this without any T cell or myeloid cell impact. We have consciously used the brain slice culture model through which the influence of systemic monocytes/macrophages as well as T cells could be excluded. Still, the net effect of tumor-derived MIF is mainly a M2 immunophenotype regardless of resident or invaded myeloid/microglial population. Furthermore, the expression of CD74 is of clinical relevance, as higher level of CD74 expression in malignant gliomas and other tumor entities is associated with a poor prognosis and correlates with resistance to the first-line chemotherapeutic agent temozolomide,^{38–40} whereas so far only one report indicates an opposite correlation based on a single-center data acquisition.⁴¹ Thus, CD74 may operate in a bidirectional manner by transmitting the MIF signal in microglial cells as well as activating a survival program within glioma cells. That CD74 can potentially promote tumor growth has been demonstrated in other malignant tumors such as lymphomas.⁴² Furthermore, targeting CD74 constitutes a strong mediator for ERK1/2 activation and protector from p53-dependent apoptosis.²⁷ CD74 can hence activate NF- κ B through intra-membrane C-terminal domain proteolysis, thereby contributing to B-cell maturation.⁴³ Here, we carried out analysis of CD74 silencing in microglial cells confirming MIF signaling as a vital tumor escape mechanism. CD74 activation inhibits microglial migration and invasion into the tumor. Knockdown of CD74 in microglia led to an increased migration toward glioma cells. Moreover, silencing MIF expression in gliomas as well as inhibiting CD74 reversed the immune-paralyzing effects on microglia and led to a reinstalled immune surveillance with recognizing the tumor core. These results could be confirmed in the *ex vivo*

Figure 4. MIF-induced microglial paralysis requires CD74 signaling. **(a)** Wild-type BV2 microglia (MG-control) and siRNA-mediated CD74 knockdown BV2 microglia (MG-siCD74) were treated with supernatants from wild-type gliomas (control), MIF knocked down gliomas (siMIF) and MIF-overexpressing gliomas (pMIF). Note that supernatants from MIF-overexpressing gliomas (pMIF) did not reduce proliferation in CD74-silenced BV2 microglia (MG-siMIF). **(b)** Wild-type microglia (green) were co-cultured in the presence of glioma cells (red) for 1 or 5 days (upper row) or CD74-silenced microglia (green) were co-cultured with glioma cells (lower row). Circled area delineates close contacts of siCD74 microglia to glioma cells. Scale bar, 12 μ m. **(c)** Quantification of tumor proliferation in the presence of wild-type microglia (control) and CD74 knocked down microglia (siCD74). **(d)** Scheme of the *ex vivo* experimental procedure OGIM. Gliomas (red) and microglial cells (green) were implanted in brain slices and tumor distance was monitored at day 1 and day 12 ($n = 7$). 2nd panel, wild-type BV2 microglia (green) at day 1 and day 12 (upper row). Distance of CD74 knockdown BV2 microglia (green) to tumor border (red) compared from day 1 with day 12 decreases (lower row). Scale bar, 2 mm. **(e)** Quantification of wild-type BV2 microglia (control) and CD74 knockdown BV2 microglia (siCD74) for migration and **(f)** tumor infiltration. **(g)** Immunohistochemical analysis of co-implanted GL261 glioma and genetically modified BV2 microglia cells in mice. Upper row: wild-type microglia (MG, green) accumulates in peritumoral areas of gliomas (red). Higher magnification of tumor border and core (20x). Lower row: CD74 knocked down microglia cells (green) are distributed within the tumor core (red). Scale bar in 'Merge' represents 3 mm and in '20x' 12 μ m. **(h)** Quantification of microglia count (in total numbers) in the tumoral (T) and peritumoral (PT) region comparing CD74-silenced group and control group. **(i)** Kaplan–Meier survival curves of glioma-implanted mice implanted with wild-type BV2 microglia (control, $n = 6$) or CD74 knockdown BV2 microglia (siCD74, $n = 6$).

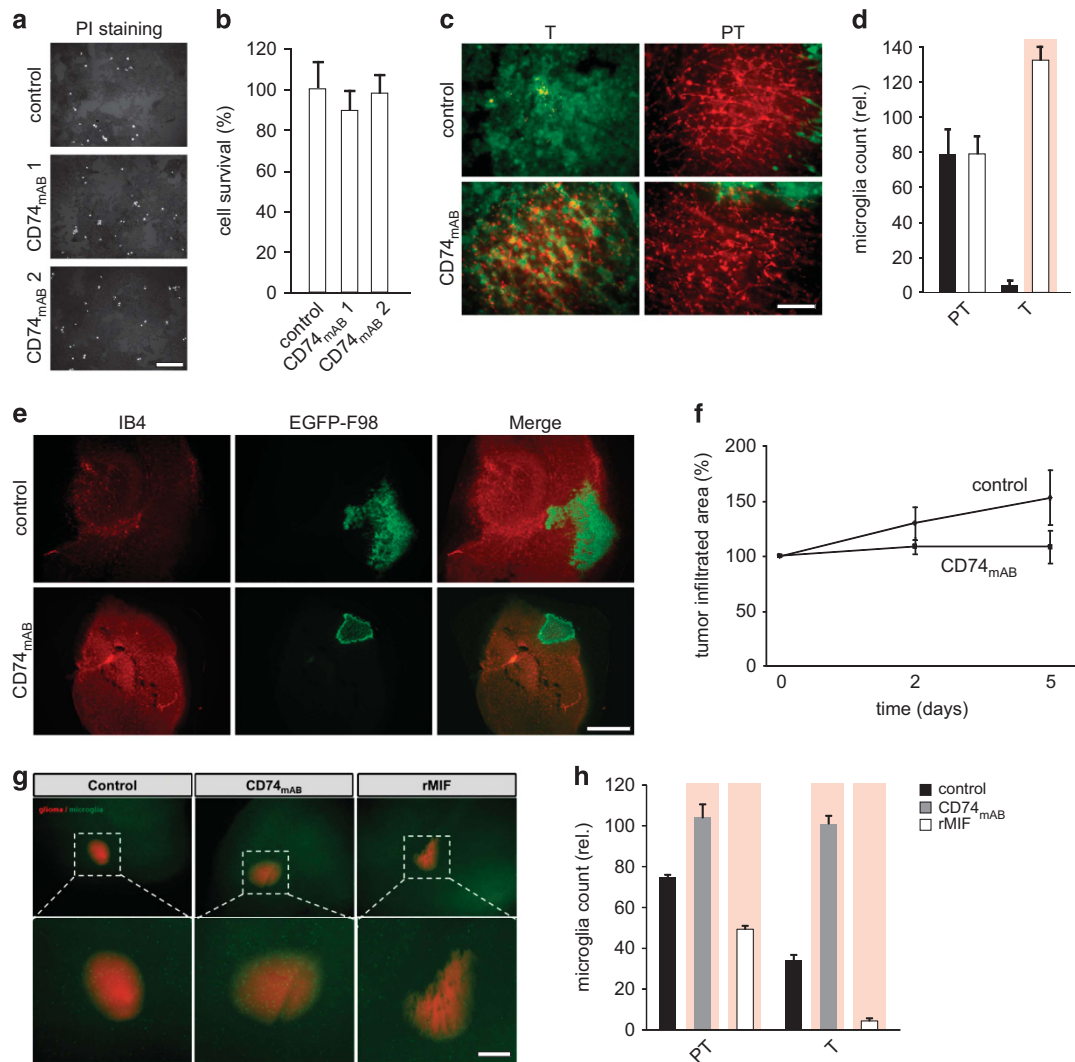


Figure 5. Modification of CD74 signal transduction on microglia reduces glioma growth. **(a)** Treatment of F98 glioma cells with two different concentrations of a monoclonal CD74 antibody (CD74_{mAB}1 and CD74_{mAB}2) for 72 h does not increase cell death, which was visualized by propidium iodide (PI) staining. Scale bar, 30 μ m. **(b)** *In vitro* F98 glioma cell survival analysis using MTT assay, control compared with monoclonal CD74 antibody treatment. **(c)** Tumor growth was measured in OGIM over a course of 5 days after tumor implantation. Image analysis of microglia in the tumor bulk and surrounding the tumor. Images show microglia staining in the tumoral and peritumoral region analyzing the difference of CD74 monoclonal antibody-treated slices and control slices. Upper row shows tumoral distribution (red) and wild-type glioma expansion (green). Lower panel shows microglial distribution in gliomas with CD74 antibody treatment. Scale bar, 15 μ m. **(d)** Quantification of microglia count (in total numbers) in the tumoral and peritumoral region comparing CD74 monoclonal antibody-treated group and control group. **(e)** Analysis of tumor growth in OGIM. Upper panel shows wild-type glioma expansion (green). Lower panel shows glioma expansion after CD74 monoclonal antibody treatment. Scale bar, 2 mm. **(f)** Quantification of tumor growth in OGIM. The growth of the tumor bulk in organotypic slices treated with a CD74 monoclonal antibody ($n = 60$) was significantly decreased compared with the control group ($n = 55$). **(g)** Brain slice cultures from CX3CR1 transgenic mice were prepared and red fluorescing GL261 glioma cells implanted (OGIM). These mice express GFP under the microglia-specific promoter CX3CR1. Slice cultures were thereafter treated with a monoclonal CD74 antibody (CD74_{mAB}) or with recombinant MIF (rMIF) over 5 days. Each group contains $n = 6$ slices. Scale bar, 2 mm. **(h)** Quantification of microglia count (in total numbers) in the tumoral and peritumoral region comparing CD74_{mAB} group, rMIF group and control group. A significant microglia accumulation is detected after CD74_{mAB} treatment in peritumoral as well as in tumoral areas. Microglia accumulation significantly decreases after rMIF treatment.

experiments. Further, we show that inhibition of tumor growth was induced before the microglial cells reached the tumor mass which implied that the tumor inhibiting effect of microglia is contact independent. We could demonstrate that disruption of MIF-CD74 signaling reinstalls microglial IFN- γ secretion. In fact, IFN- γ is a potent anti-tumor effector molecule supported by the findings that numerous tumor entities display an inactivating mutation in the IFN- γ signaling pathway, through which tumor cells escape immune control. On the contrary, interference with the MIF-CD74 axis leads to a rescue, through which IFN- γ

was reinstalled and secreted, leading to dramatic inhibition of tumor progression. In addition, treatment of malignant gliomas with clinically feasible concentrations of IFN- γ led to reduced tumor growth. Although IFN- γ has direct glioma growth-inhibitory effects, it is also known to affect M1/M2 polarization of microglia.⁴⁴ In this context we could show that MIF-CD74-dependent M2 polarization of glioma-associated microglia is controlled by silencing microglial IFN- γ expression. Interference with MIF-CD74 pathway diminishes this effect and allows microglia to polarize into a M1 phenotype hindering

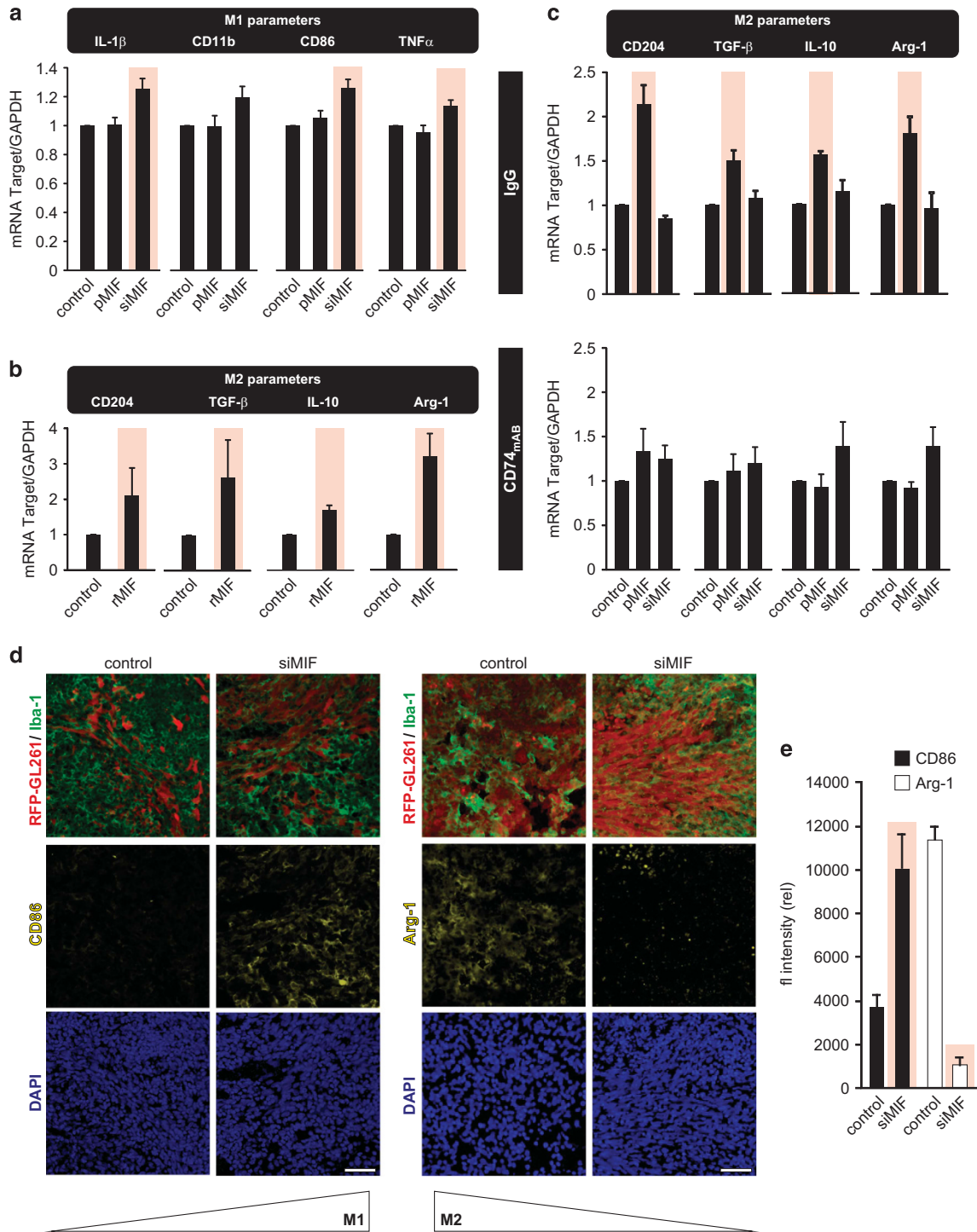


Figure 6. MIF shifts microglia into a M2 phenotype. **(a)** Analysis of M1 parameters in co-cultivated BV2 microglia cells with genetically modified GL261 glioma cells ($n=3$). Co-cultures contain a semi-permeable membrane, which separates both cell entities. After 20 h co-culture BV2 microglia were analyzed for expression of M1 markers by quantitative RT-PCR. Almost all M1 parameters significantly increase in their expression in BV2 microglia after co-culture with MIF over-secreting GL261 glioma cells, whereas siRNA-silenced GL261 glioma cells do not. **(b)** M2 markers in primary murine microglia were analyzed by quantitative RT-PCR after rMIF treatment ($n=3$). 20 h of rMIF treatment significantly increases expression of M2 parameters (that is, CD204, TGF- β , IL-10 and Arg-1). **(c)** Analysis of M2 parameters in co-cultivated BV2 microglia cells with genetically modified GL261 glioma cells ($n=3$). Co-cultures contain a semi-permeable membrane, which separates both cell entities. After 20 h co-culture BV2 microglia were analyzed for expression of M2 markers by quantitative RT-PCR. M2 parameters significantly increase in their expression in BV2 microglia after co-culture with MIF over-secreting GL261 glioma cells, whereas siRNA-silenced GL261 glioma cells do not. **(d)** Analysis of microglial shift *in vivo*. Brain sections of GL261 (red) implanted mice were analyzed for expression of the M1 and M2 markers (yellow) CD86 and Arg-1. Nuclei were stained by DAPI (blue). Total microglia staining was performed by Iba-1 staining (green). Left column, CD86 as a representative marker for M1 polarization was dramatically increased in MIF-silenced gliomas compared with wild-type MIF-expressing glioma cells. Right column, Arg-1 as a representative marker for M2 polarization was conversely decreased in MIF-silenced gliomas compared with wild-type MIF-expressing gliomas. Scale bar, 20 μ m. **(e)** Quantitative analysis of CD86 (black) and Arg-1 (white) staining through measurement of fluorescence intensities.

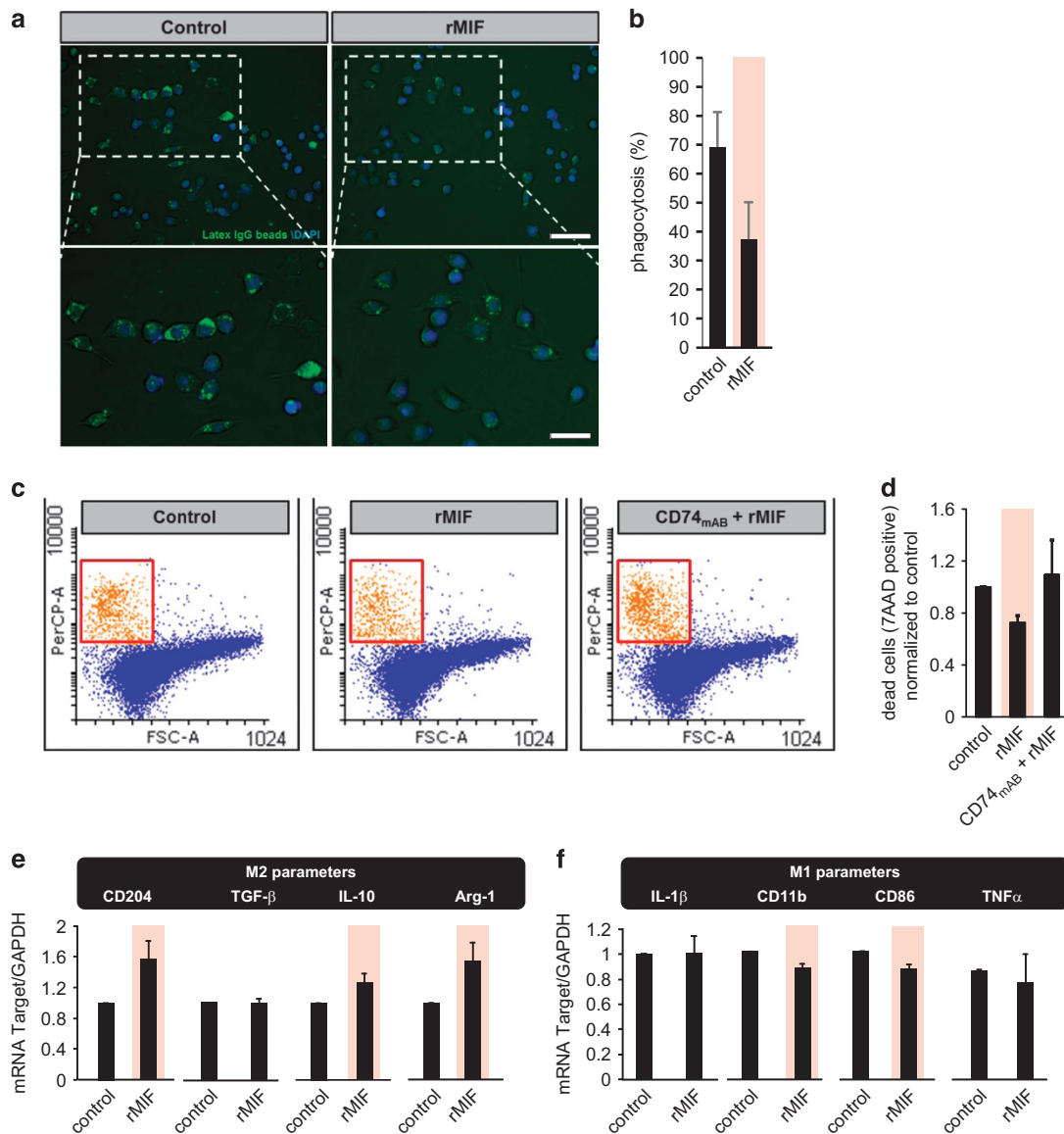


Figure 7. MIF modulates phagocytotic activity and cytotoxic potency of microglia. **(a)** Phagocytotic activity after 24 h of rMIF treatment was analyzed. To visualize phagocytosis primary murine microglia were fed with green fluorescent latex IgG beads. Scale bar, 15 μ m. **(b)** Quantification of microglial phagocytotic activity (green fluorescent microglia in relation to total microglia in %; $n = 4$). Treatment with rMIF significantly decreases microglial phagocytosis. **(c)** FACS analysis of microglial cytotoxicity ($n = 3$ repetitions). Primary murine microglia were co-cultured with GL261 glioma cells. Co-cultures contain a semi-permeable membrane, which separates both cell entities. Three days after cultivation only GL261 glioma cells were analyzed by FACS. **(d)** Quantification of 7AAD-positive glioma cells shows a significantly reduced amount of dead glioma cells after rMIF treatment, whereas a combination of CD74_{mAB} plus rMIF diminishes this effect. **(e)** Analysis of M2 parameters by quantitative RT-PCR of phagocytosing microglia which were fed with green fluorescent latex IgG beads. Treatment of BV2 microglia with recombinant MIF leads to significantly increased expression of almost all M2 parameters. **(f)** Analysis of M1 parameters by quantitative RT-PCR of phagocytosing microglia which were fed with green fluorescent latex IgG beads. Treatment of BV2 microglia with recombinant MIF leads to significantly decreased expression of CD11b and CD86 as prominent M1 markers.

further glioma growth. This novel finding expands the mode of MIF action in addition to a direct polarizing effect via CD74. Here, we demonstrate that in addition to its anti-tumoral effects IFN- γ can also shift microglial polarization toward M1 activation. IFN- γ has been known to stimulate MIF secretion in immunocompetent cells.⁴⁵ Our data shows that MIF treatment suppresses IFN- γ secretion, which can be attributed to a negative feedback mechanism. In addition, current studies concur with our data that MIF is an immunosuppressive cytokine, which inhibits activation of tumor-associated macrophages in other cancer entities.⁴⁶

These findings have several clinical implications. First, there is a correlation of microglial accumulation in gliomas and their malignancy, making microglia and the tumor microenvironment a potential biomarker target. Secondly, we found that inhibition of MIF and CD74 can abrogate the tumor escape mechanism and foster anti-glioma activity. Since clinical phase I trials with humanized MIF and CD74 neutralizing antibodies showed no adverse side effects,⁴⁷ inhibition of MIF and CD74 in glioma patients is well conceivable. Further, our study indicates that shifting microglial cells toward M1 activation status is a viable approach in normalizing the tumor microenvironment and thereby attenuating tumor growth.

MATERIALS AND METHODS

Cell lines

Murine GL261 glioma and BV2 microglia cell lines, rat glioma cell line F98 and human glioma cell line U87MG were cultured in DMEM (Dulbecco's modified Eagle's medium; Gibco Life Technologies, Darmstadt, Germany) medium containing 10% fetal calf serum (Biochrom, Berlin, Germany) and antibiotics (Gibco) in humidified atmosphere at 37 °C and 5% CO₂. Cell lines were transfected using Roti-Fect (Carl Roth GmbH, Karlsruhe, Germany) according to the manufacturer's protocol.

Proliferation assays

BrdU assays were performed according to the manufacturer's protocol (Roche Applied Sciences, Mannheim, Germany). For MTT proliferation cells were incubated with 400 µg/ml MTT for 6 h before the medium was discarded and cells were resuspended in Isopropanol plus 0.04 M HCl. After mixing, this solution was measured in an ELISA reader at 550 nm; a reference wavelength of 690 nm was used.

Immunofluorescence staining

Brains are fixated with 4% para-formaldehyde (Merk, Germany) including 5% sucrose (Roche Applied Sciences) for 24 h, followed by cryoprotection in 30% (wt/vol) sucrose in 0.1 M phosphate-buffered saline (PBS) for 2–3 days. After freezing brains in tissue-Tek, brains are cut and processed free-floating for primary antibodies and immunofluorescence staining. Sections are incubated for 30 min with 0.5% Triton X (Sigma-Aldrich, Taufkirchen, Germany) in PBS, followed by primary antibody incubation in 3% horse serum or fetal calf serum and 0.2% Triton X-100 as the blocking solution and subsequently incubated overnight at 4 °C. Alexa Fluor 448, 568 and 647 (Invitrogen/Life Technologies) were used as secondary antibodies with 1:1000 concentration. Sections were then washed three times in PBS, stained with Hoechst (Invitrogen/Life Technologies). These stained tissue slices were then flat-mounted with ImmuMount (Thermo Scientific, Schwerte, Germany).

Primary murine microglia

To obtain pre-labeled primary microglia we used the microglial reporter mouse strain CX3CR1^{GFP},⁴⁸ and microglial cells were isolated as described with minor modifications.⁴⁹ Cerebral cortices from mice postnatal day 3 were dissected, carefully stripped of their meninges, digested with 0.25% trypsin and dispersed into a single-cell level. The cell suspension ('mixed glia') was then cultured at 37 °C in humidified 5% CO₂, 95% air. Medium was replaced every 4–5 days. Mixed glia cultures reached confluence after 7–10 days and were used to harvest microglia between 15 and 20 days after preparation. Microglia cells were isolated by mild trypsinization (mild T/E). Briefly, treatment of the confluent mixed glial cultures with 0.06% trypsin (mild T/E) resulted in detachment of an intact layer of cells containing almost all the astrocytes and leaving behind a highly enriched population of microglia (>98%, as determined by CX3CR1-GFP). The attached microglia were allowed to recover for 24 h.

Primary human microglia

Human brain tissues were obtained at the University of Erlangen (Germany) in accordance with the local ethical review board and processed within 2 h after surgery. Isolation of microglia was performed according to published protocols with some modification.⁵⁰ Human brain tissues were obtained at the University of Erlangen (Germany) in accordance with the local ethical review board and processed within 2 h after surgery. Isolation of microglia was performed according to published protocols with some modification. Tissue was enzymatically digested with 10 ml/g of tissue of HBSS with papain (2.5 U/ml; Worthington, Lakewood, NJ, USA) and DNase (10 U/ml; Roche, Freiburg, Germany) for 1 h at 37 °C and filtrated with a 100-µm cell strainer (BD Falcon, Germany). The cell suspension was then cultured at 37 °C in humidified 5% CO₂, 95% air. Medium was replaced every 4 days. The isolation of microglia were performed by shaking (90 min) and afterwards isolated microglia were transferred to 6-well-plates. Attached microglia were allowed to recover for 24 h prior experimentation.

Co-culture

For co-culture experiments 2 × 10⁵ microglia cells were cultured for 2 h. Thereafter, 15 × 10⁴ MIF-overexpressing or knockdown F98 cells were

seeded on a membrane and were co-cultured for 3 days. Co-cultures contain a semi-permeable membrane, which separates both cell entities. Then, cells were lysed with TRI reagent (Sigma, Taufkirchen, Germany) according to the manufacturer's protocol for RNA isolation.

Protein analyses

Western blot analysis was performed according to the manufacturer's manual (NUPAGE, Invitrogen Life Technologies, Darmstadt, Germany). For total protein extraction, cell pellets were resuspended in lysis buffer containing 50 mM Tris-HCl (pH 8, Sigma), 150 mM NaCl (Merck, Darmstadt, Germany), 1% Triton X-100 (Sigma-Aldrich), 0.1% SDS (Sigma-Aldrich), 1 mM EDTA (pH 8, Merck), 1 mM phenylmethylsulfonyl fluoride (PMSF, Roche) and 1 protease inhibitor tablet (Roche). After centrifugation at 15 000 g for 10 min at 4 °C, supernatant was subjected to SDS-polyacrylamide gel electrophoresis on a 12% polyacrylamide gel. Twenty micrograms of the soluble fraction were loaded per lane. The separated proteins were electro-blotted onto a nitrocellulose membrane (Sigma-Aldrich). Equal loading amounts of the probes were estimated using immunostaining with anti-mouse β-actin (Sigma-Aldrich) or GAPDH (Abcam, Berlin, Germany) monoclonal antibodies. Cells were analyzed for the MIF (Torrey Pines Biolabs, Secaucus, NJ, USA), CD74 (Santa Cruz Biotechnology, Heidelberg, Germany), ERK1/2 and pERK1/2 (Cell Signaling Technology, Danvers, MA, USA) with respective antibodies and the chemiluminescence method (Amersham, Munich, Germany) according to the manufacturer's protocol.

Live image video microscopy and OGIM

Brain slice cultures and glioma imaging were prepared and maintained as described.^{4,51} After decapitation, brains of 4-day-old Wistar rats were rapidly removed and placed into ice-cold preparation medium. The brains were cut in 350 µm thick horizontal slices in preparation medium and cultured in humidified atmosphere at 35 °C and 5% CO₂ according to the interphase technique in culture medium. The medium was changed 1 day after preparation and every second day thereafter. Stably GFP-or RFP-transfected F98 or GL261 glioma cells and BV2 microglial cells were implanted within a total volume of 0.1 µl medium into the slice 1 day after slice preparation. One day after implantation and every second day, glioma growth and invasion were evaluated using an inverse fluorescence microscope (BX51 microscope; Olympus).

MRI

MR imaging was performed on a 3 Tesla MR scanner unit (Magnetom Trio, Siemens Healthcare, Erlangen, Germany) with a 40-mm-diameter, small field-of-view orbit surface coil as receiver. Scout images and a 3DCISS sequence (repetition time = 9 ms, echo time = 5 ms, reconstructions with a slice thickness of 0.4 mm) were obtained in coronal, axial and transverse planes to position the slices accurately. Ten coronal T1-weighted slices, each with 1 mm thickness and 0.2 mm separation (inter-slice gap) were then positioned on the transverse scout images to cover the tumor. T1-weighted images were acquired with a 256x256 matrix, field-of-view = 40 mm, repetition time = 507 ms, echo time = 17 ms, and a total scan time of 3 min 42 s. For contrast-enhanced images, each animal received 1 ml/kg body weight of contrast agent (Gadovist 1M, Bayer Vital GmbH, Leverkusen, Germany) i.p. 10 min before the acquisition of T1-weighted sequences. Imaging analysis was performed for each animal on the central slices using Siemens build-in image processing software to outline tumor volume on the T1-weighted contrast-enhanced images. Total tumor volume was calculated as the summed area on all slices, multiplied by the slice separation and compared to histology-derived tumor volume.

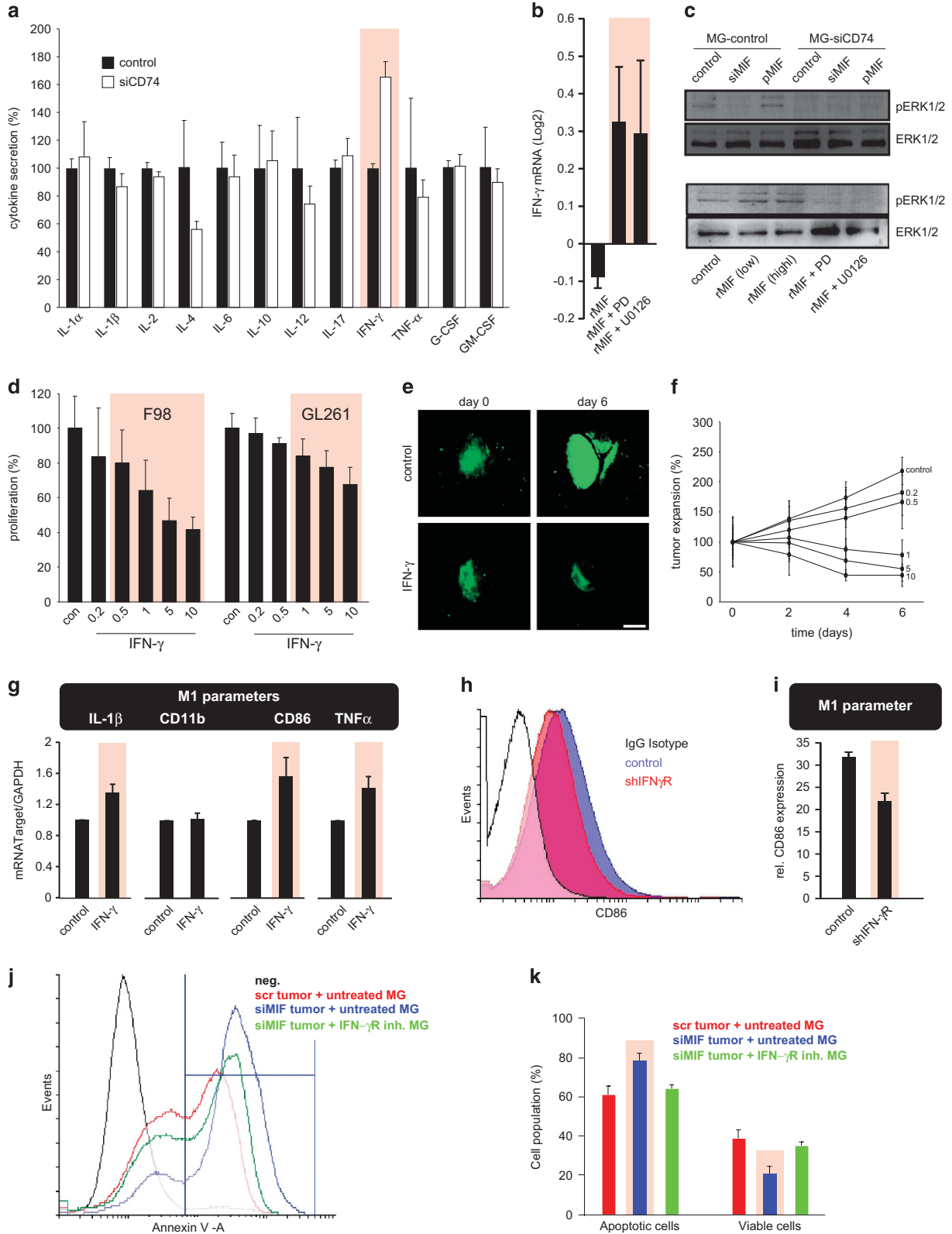
Genetically modified cells

The following plasmids were used to genetically modify each cell line: pEGFP-N1 (Clontech Laboratories Inc., Mountain View, CA, USA), pSuper-neo+GFP (Oligoengine, Seattle, WA, USA), pIRES2-AcGFP (Clontech Laboratories Inc.), pmRFP-C based on pEGFP-C2. For MIF overexpression the plasmid pIRES2-AcGFP containing the mouse-MIF sequence NM_010798 was used. MIF, CD74 and INFγR1 knockdowns were performed by RNA interference using the pSuper system. Necessary inserts based on NM_010798 (MIF), NM_010545 (CD74) and NM_010511.2 (INFγR1).

ELISA

To measure MIF secretion, MIF ELISA kit from MyBiosource (cat. no: MBS296978) company based on biotin double antibody sandwich technology was used. Supernatants of MIF overexpress and knockdown cells were added to wells that are pre-coated with MIF monoclonal

antibody. After 30 min incubation, MIF antibody and streptavidin-HRP were added and incubated for 60 min at 37 °C. After five times of washing, chromogen solution A and B were added and incubated for 10 min at 37 °C for color development. After incubation, stop solution was added to measure the absorbance under 450 nm wavelength.



Gene expression analysis

Total RNA was extracted using TRI reagent (Sigma) according to the manufacturer's protocol. cDNA was synthesized with 1 µg of total RNA using Thermo Scientific Reverse Transcription according to the

manufacturer's protocol. Real-time (SYBR Green) PCR was performed in a LightCycler 480 (Roche Applied Sciences) according to the manufacturer's protocol (Thermo Scientific). All samples were assessed in relation to the levels of GAPDH expression as an internal control. Q-PCR data were assessed and reported according to the $\Delta\Delta C_t$ method.

Xenograft studies

Tumors were implanted into the right frontal lobe of C57BL/6 mice (Charles River, Sulzfeld, Germany). The animals were anesthetized by intraperitoneal injection of 500 µl of a mixture of ketamine (Pharmacia GmbH, Erlangen, Germany), xylazine (Bayer Health Care, Hetzles, Germany) and atropine (Braun, Melsungen, Germany) and placed in a fixations frame (David Kopf Instruments, Tujunga, CA, USA). GL261 glioma cells (6×10^4) were implanted into the right frontal lobe of the animals (0 mm AP, 2 mm lateral to bregma, depth 3 mm from dura). For co-implantation RFP-marked GL261 cells were implanted into the right frontal lobe of C57BL/6 mice as described above. Tumor growth was confirmed by MR imaging at 10 days after implantation. Tumor positive individuals received co-implantation of 6×10^4 GFP-expressing BV2 microglia cells 2 mm posterior to the tumor.

Phagocytosis assay

Microglia cells (2×10^4) were cultured in 24 wells plate. After 12 h, cells were treated with 100 ng/ml rMIF or PBS as control. Latex Beads-Rabbit IgG-FITC complex (Cayman, cat. no. 400291) was added for 24 h. To prepare a Latex Beads-Rabbit IgG-FITC solution, beads solution were diluted 1:1000 according to manufacturer's protocol.

Boyden chamber assay

Migration assays were performed using Boyden chambers according to the manufacturer's protocol (Millipore, Billerica, MA, USA). Per assay 2.5×10^5 cells were plated into each chamber and incubated for 24 h.

FACS

To quantify glioma cell death under microglia co-culture, F98 cells were cultured (2×10^5 cells per 6-well plate). After 2 h, microglia cells (15×10^4 cells) were seeded on the membrane and treated with rMIF (100 ng/ml) or CD74 antibody (1 µg/ml; Santa Cruz Biotechnology, cat. no. SC-5438). After 3 days incubation, F98 cells were trypsinized and 1 µl/ml 7AAD or Annexin V (Invitrogen/Life Technologies) were used for cell death analysis with BD FACSCantoTM II.

Patient samples

Surgical specimens examined in this study were histologically diagnosed as glioblastoma multiforme (WHO^{IV}), anaplastic astrocytoma (WHO^{III}), diffuse astrocytoma (WHO^{II}) or juvenile pilocytic astrocytoma (WHO^I) according to the WHO classification. Human neocortex negative for human

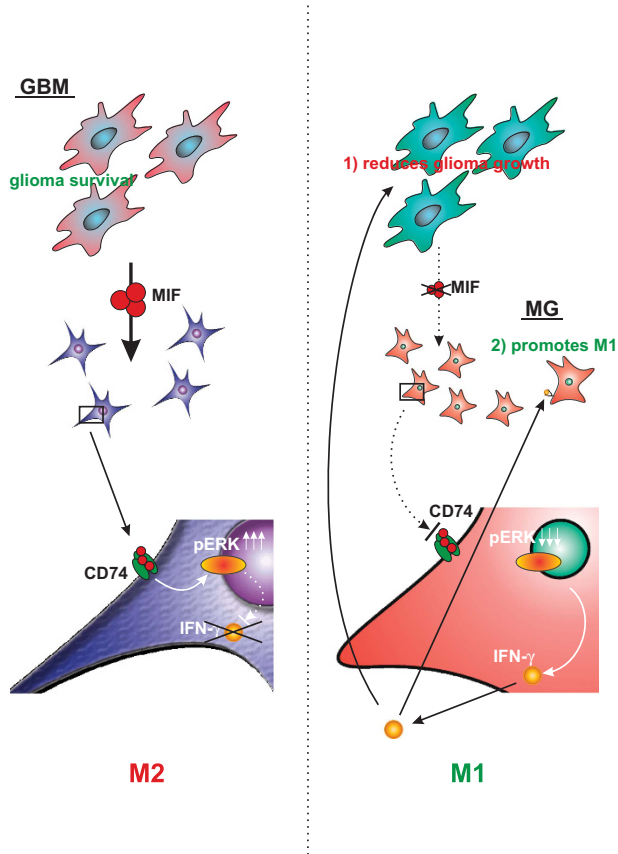


Figure 9. Interaction of malignant glioma cells and microglia. Schematic summary of experimental data revealed that malignant brain tumors secrete the cytokine MIF, which activates the CD74 receptor on microglial cells. This results in tumor immune escape with paralyzing microglial anti-glioma activity. However, influencing this signal pathway either by MIF inhibition or by CD74 receptor inactivation reinstates microglial immune surveillance activity. This M2 into a M1 phenotype shift goes along with IFN-γ secretion and consecutively leads to tumor cell death.

Figure 8. MIF inhibits IFN-γ secretion. (a) Supernatants from wild-type BV2 microglia (control) and CD74 knockdown BV2 microglia (siCD74) were profiled by cytokine ELISA ($n = 3$). CD74 knockdown microglia show elevated IFN-γ secretion. (b) Primary murine microglia were treated with rMIF or inhibitors of the MAPK signaling pathway (PD or U0126). Treatment with rMIF-silenced IFN-γ expression. Treatment with PD or U0126 diminished this effect and a significantly increased microglial expression of IFN-γ is detectable. (c) Upper panel, glioma-derived MIF secretion activates microglial ERK1/2 via CD74 receptor. Wild-type primary murine microglial cells (MG-control) and CD74 knocked down microglia (MG-siCD74) were treated with supernatants from wild-type gliomas (control), MIF knocked down gliomas (siMIF), and MIF-overexpressing gliomas (pMIF) and phosphorylated ERK1/2 was detected by immunoblotting. Total ERK1/2 serves as a loading control. Lower blot, BV2 microglial cells were treated with two different concentrations of rMIF, the ERK inhibitor PD98059 (PD) or the MEK inhibitor U0126. Phosphorylated ERK1/2 was detected after rMIF treatment, whereas both inhibitors suppressed ERK1/2 phosphorylation. Total ERK1/2 serves as a loading control. (d) Rodent (F98) and murine gliomas (GL261) were treated with various concentrations of IFN-γ for 5 days and proliferation was determined by MTT ($n = 7$). Treatment reduced dose-dependent glioma proliferation significantly. (e) Tumor-implanted brain slices were treated with various concentration of IFN-γ (0.2–10 ng/ml) and tumor occupied areas were monitored after 0, 2, 4 and 6 days. Scale bar, 2 mm. (f) Quantification of tumor growth in OGIM after IFN-γ treatment. (g) M1 markers in primary murine microglia were analyzed by quantitative RT-PCR after IFN-γ treatment ($n = 3$). 20 h of IFN-γ treatment significantly increases expression of M1 parameters (that is, IL-1β, CD86, TNFα), whereas CD11b was not affected. (h) Analysis of IFN-γ receptor inhibition by FACS. (i) Quantitative analysis of FACS data. Short hairpin-mediated silencing of IFN-γ receptor significantly decreases M1 polarization (CD86 as a representative M1 marker) compared with control microglia. (j) Co-cultures of MIF-silenced glioma cells either with wild-type microglia or IFN-γ receptor silenced microglia were analyzed by FACS following annexin V-A staining to identify microglial ability to induce glioma cell death. (k) Quantitative analysis of FACS data. Wild-type microglial cells kill MIF-silenced glioma cells. This effect was completely negated following silencing of microglial IFN-γ receptor.

brain tumors served as a control. Patients underwent surgical treatment in the Department of Neurosurgery of the University of Erlangen-Nürnberg, Germany.

Ethical statements

Studies with human tissue were conducted in compliance with the Helsinki Declaration and approved by the Ethics Committee of the Friedrich Alexander University of Erlangen-Nuremberg. All patients gave written informed consent to participate in the study.

Animal killing was performed in accordance with the German Protection of Animals Act 14 paragraph one and three. The announcement of rat and mouse killing was approved by the designer for animal protection of the University of Erlangen-Nuremberg (TS-7/12).

Animal experiments were done in congruence with the European Union guidelines for the use of laboratory animals. The protocol for animal experimentation was approved by the Government of Central Franconia (permission number 54.2531.31-8/06).

Statistics

Significant differences in figures are colored in pink. Data are given as value means \pm s.e.m. Significance is given as confidence intervals at the 95% confidence level with $P < 0.05$ (student's *t*-test) if not otherwise stated. For Kaplan–Meier survival curves, statistical analysis was performed by Log-rank test (Figure 2: $P < 0.0005$; Figure 4: $P < 0.0179$).

CONFLICT OF INTEREST

The authors declare no conflict of interest.

ACKNOWLEDGEMENTS

Our work is supported by the German Research Foundation (DFG Ey 94/2-1).

AUTHOR CONTRIBUTIONS

NES and IYE conceived and designed the study. AG and MAS performed all experiments. MAS and TE contributed to the *in vivo* experiments and MR imaging analysis under the supervision of AD, MAS, AG, TE, RB and MB analyzed and interpreted the data and discussed the data with all authors. NES and IYE wrote the manuscript. All authors contributed to the preparation of the final manuscript. AG performed the present work in fulfillment of the requirements for obtaining the degree Dr rer. biol. hum. at the Friedrich Alexander University of Erlangen-Nürnberg (FAU).

REFERENCES

- Dunn GP, Rinne ML, Wykosky J, Genovese G, Quayle SN, Dunn IF et al. Emerging insights into the molecular and cellular basis of glioblastoma. *Genes Dev* 2012; **26**: 756–784.
- Jain RK, di Tomaso E, Duda DG, Loeffler JS, Sorensen AG, Batchelor TT. Angiogenesis in brain tumours. *Nat Rev Neurosci* 2007; **8**: 610–622.
- Rao JS. Molecular mechanisms of glioma invasiveness: the role of proteases. *Nat Rev Cancer* 2003; **3**: 489–501.
- Savaskan NE, Heckel A, Hahnen E, Engelhorn T, Doerfler A, Ganslandt O et al. Small interfering RNA-mediated xCT silencing in gliomas inhibits neurodegeneration and alleviates brain edema. *Nat Med* 2008; **14**: 629–632.
- Saadoun S, Papadopoulos MC. Aquaporin-4 in brain and spinal cord oedema. *Neuroscience* 2010; **168**: 1036–1046.
- Lyons SA, Chung WJ, Weaver AK, Ogunrinu T, Sontheimer H. Autocrine glutamate signaling promotes glioma cell invasion. *Cancer Res* 2007; **67**: 9463–9471.
- Savaskan NE, Seufert S, Hauke J, Trankle C, Eyupoglu IY, Hahnen E. Dissection of mitogenic and neurodegenerative actions of cystine and glutamate in malignant gliomas. *Oncogene* 2011; **30**: 43–53.
- Engelhorn T, Savaskan NE, Schwarz MA, Kreutzer J, Meyer EP, Hahnen E et al. Cellular characterization of the peritumoral edema zone in malignant brain tumors. *Cancer Sci* 2009; **100**: 1856–1862.
- Zhai H, Heppner FL, Tsirka SE. Microglia/macrophages promote glioma progression. *Glia* 2011; **59**: 472–485.
- Eyupoglu IY, Bechmann I, Nitsch R. Modification of microglia function protects from lesion-induced neuronal alterations and promotes sprouting in the hippocampus. *FASEB J* 2003; **17**: 1110–1111.

- Ullrich O, Diestel A, Eyupoglu IY, Nitsch R. Regulation of microglial expression of integrins by poly(ADP-ribose) polymerase-1. *Nat Cell Biol* 2001; **3**: 1035–1042.
- Heneka MT. Macrophages derived from infiltrating monocytes mediate autoimmune myelin destruction. *J Exp Med* 2014; **211**: 1500.
- Komohara Y, Takemura K, Lei XF, Sakashita N, Harada M, Suzuki H et al. Delayed growth of EL4 lymphoma in SR-A-deficient mice is due to upregulation of nitric oxide and interferon-gamma production by tumor-associated macrophages. *Cancer Sci* 2009; **100**: 2160–2166.
- Komohara Y, Horlad H, Ohnishi K, Fujiwara Y, Bai B, Nakagawa T et al. Importance of direct macrophage-tumor cell interaction on progression of human glioma. *Cancer Sci* 2012; **103**: 2165–2172.
- Prośniak M, Harshyne LA, Andrews DW, Kenyon LC, Bedelbaeva K, Apanasovich TV et al. Glioma grade is associated with the accumulation and activity of cells bearing M2 monocyte markers. *Clin Cancer Res* 2013; **19**: 3776–3786.
- Ku MC, Wolf SA, Respondek D, Matyjasz V, Pohlmann A, Waiczies S et al. GDNF mediates glioblastoma-induced microglia attraction but not astrogliosis. *Acta Neuropathol* 2013; **125**: 609–620.
- Pyonteck SM, Akkari L, Schuhmacher AJ, Bowman RL, Sevenich L, Quail DF et al. CSF-1 R inhibition alters macrophage polarization and blocks glioma progression. *Nat Med* 2013; **19**: 1264–1272.
- Sielska M, Przanowski P, Wylot B, Gabrusiewicz K, Maleszewska M, Kijewska M et al. Distinct roles of CSF family cytokines in macrophage infiltration and activation in glioma progression and injury response. *J Pathol* 2013; **230**: 310–321.
- Wesolowska A, Kwiatkowska A, Slomnicki L, Dembinski M, Master A, Sliwa M et al. Microglia-derived TGF-beta as an important regulator of glioblastoma invasion—an inhibition of TGF-beta-dependent effects by shRNA against human TGF-beta type II receptor. *Oncogene* 2008; **27**: 918–930.
- Bernhagen J, Krohn R, Lue H, Gregory JL, Zernecke A, Koenen RR et al. MIF is a noncognate ligand of CXC chemokine receptors in inflammatory and atherogenic cell recruitment. *Nat Med* 2007; **13**: 587–596.
- Binsky I, Haran M, Starlets D, Gore Y, Lantner F, Harpaz N et al. IL-8 secreted in a macrophage migration-inhibitory factor- and CD74-dependent manner regulates B cell chronic lymphocytic leukemia survival. *Proc Natl Acad Sci USA* 2007; **104**: 13408–13413.
- Calandra T, Rogier T. Macrophage migration inhibitory factor: a regulator of innate immunity. *Nat Rev Immunol* 2003; **3**: 791–800.
- Leng L, Metz CN, Fang Y, Xu J, Donnelly S, Baugh J et al. MIF signal transduction initiated by binding to CD74. *J Exp Med* 2003; **197**: 1467–1476.
- Ren Y, Chan HM, Li Z, Lin C, Nicholls J, Chen CF et al. Upregulation of macrophage migration inhibitory factor contributes to induced N-Myc expression by the activation of ERK signaling pathway and increased expression of interleukin-8 and VEGF in neuroblastoma. *Oncogene* 2004; **23**: 4146–4154.
- Rhodes DR, Yu J, Shanker K, Deshpande N, Varambally R, Ghosh D et al. ONCOMINE: a cancer microarray database and integrated data-mining platform. *Neoplasia* 2004; **6**: 1–6.
- Lubetsky JB, Dios A, Han J, Aljabari B, Ruzsicska B, Mitchell R et al. The tautomerase active site of macrophage migration inhibitory factor is a potential target for discovery of novel anti-inflammatory agents. *J Biol Chem* 2002; **277**: 24976–24982.
- Shi X, Leng L, Wang T, Wang W, Du X, Li J et al. CD44 is the signaling component of the macrophage migration inhibitory factor-CD74 receptor complex. *Immunity* 2006; **25**: 595–606.
- Fingerle-Rowson G, Kaleswarapu DR, Schlander C, Kabgani N, Brocks T, Reinart N et al. A tautomerase-null macrophage migration-inhibitory factor (MIF) gene knock-in mouse model reveals that protein interactions and not enzymatic activity mediate MIF-dependent growth regulation. *Mol Cell Biol* 2009; **29**: 1922–1932.
- Eyupoglu IY, Buchfelder M, Savaskan NE. Surgical resection of malignant gliomas—role in optimizing patient outcome. *Nat Rev Cancer* 2013; **9**: 141–151.
- Hanahan D, Weinberg RA. Hallmarks of cancer: the next generation. *Cell* 2011; **144**: 646–674.
- Joyce JA, Pollard JW. Microenvironmental regulation of metastasis. *Nat Rev Cancer* 2009; **9**: 239–252.
- Baron N, Deuster O, Noelker C, Stuer C, Strik H, Schaller C et al. Role of macrophage migration inhibitory factor in primary glioblastoma multiforme cells. *J Neurosci Res* 2011; **89**: 711–717.
- Mittelbronn M, Platten M, Zeiner P, Dombrowski Y, Frank B, Zachskorn C et al. Macrophage migration inhibitory factor (MIF) expression in human malignant gliomas contributes to immune escape and tumour progression. *Acta Neuropathol* 2011; **122**: 353–365.
- Schwartz V, Lue H, Kraemer S, Korbil J, Krohn R, Ohl K et al. A functional heteromeric MIF receptor formed by CD74 and CXCR4. *FEBS Lett* 2009; **583**: 2749–2757.
- Bryan KJ, Zhu X, Harris PL, Perry G, Castellani RJ, Smith MA et al. Expression of CD74 is increased in neurofibrillary tangles in Alzheimer's disease. *Mol Neurodegener* 2008; **3**: 13.

- 36 Flynn G, Maru S, Loughlin J, Romero IA, Male D. Regulation of chemokine receptor expression in human microglia and astrocytes. *J Neuroimmunol* 2003; **136**: 84–93.
- 37 Muller A, Brandenburg S, Turkowski K, Muller S, Vajkoczy P. Resident microglia, and not peripheral macrophages, are the main source of brain tumor mononuclear cells. *Int J Cancer* 2015; **137**: 278–288.
- 38 Butrym A, Majewski M, Dzierzyczenia J, Kuliczkowski K, Mazur G. High CD74 expression correlates with ZAP70 expression in B cell chronic lymphocytic leukemia patients. *Med Oncol* 2013; **30**: 560.
- 39 Kitange GJ, Carlson BL, Schroeder MA, Decker PA, Morlan BW, Wu W *et al*. Expression of CD74 in high grade gliomas: a potential role in temozolomide resistance. *J Neurooncol* 2010; **100**: 177–186.
- 40 Nagata S, Jin YF, Yoshizato K, Tomoeda M, Song M, Iizuka N *et al*. CD74 is a novel prognostic factor for patients with pancreatic cancer receiving multimodal therapy. *Ann Surg Oncol* 2009; **16**: 2531–2538.
- 41 Zeiner PS, Preusse C, Blank AE, Zachskorn C, Baumgarten P, Caspary L *et al*. MIF receptor CD74 is restricted to microglia/macrophages, associated with a M1-polarized immune milieu, and prolonged patient survival in gliomas. *Brain Pathol* 2015; **25**: 491.
- 42 Gupta P, Goldenberg DM, Rossi EA, Cardillo TM, Byrd JC, Muthusamy N *et al*. Dual-targeting immunotherapy of lymphoma: potent cytotoxicity of anti-CD20/CD74 bispecific antibodies in mantle cell and other lymphomas. *Blood* 2012; **119**: 3767–3778.
- 43 Becker-Herman S, Arie G, Medvedovsky H, Kerem A, Shachar I. CD74 is a member of the regulated intramembrane proteolysis-processed protein family. *Mol Biol Cell* 2005; **16**: 5061–5069.
- 44 Wei J, Gabrusiewicz K, Heimberger A. The controversial role of microglia in malignant gliomas. *Clin Dev Immunol* 2013; **2013**: 285246.
- 45 Calandra T, Bernhagen J, Mitchell RA, Bucala R. The macrophage is an important and previously unrecognized source of macrophage migration inhibitory factor. *J Exp Med* 1994; **179**: 1895–1902.
- 46 Yaddanapudi K, Rendon BE, Lamont G, Kim EJ, Al Rayyan N, Richie J *et al*. MIF is necessary for late-stage melanoma patient MDSC immune suppression and differentiation. *Cancer Immunol Res* 2015; **4**: 101–112.
- 47 Kaufman JL, Niesvizky R, Stadtmauer EA, Chanan-Khan A, Siegel D, Horne H *et al*. Phase I, multicentre, dose-escalation trial of monotherapy with milatuzumab (humanized anti-CD74 monoclonal antibody) in relapsed or refractory multiple myeloma. *Br J Haematol* 2013; **163**: 478–486.
- 48 Jung S, Aliberti J, Graemmel P, Sunshine MJ, Kreutzberg GW, Sher A *et al*. Analysis of fractalkine receptor CX(3)CR1 function by targeted deletion and green fluorescent protein reporter gene insertion. *Mol Cell Biol* 2000; **20**: 4106–4114.
- 49 Saura J, Tusell JM, Serratosa J. High-yield isolation of murine microglia by mild trypsinization. *Glia* 2003; **44**: 183–189.
- 50 Smith AM, Gibbons HM, Lill C, Faull RL, Draganow M. Isolation and culture of adult human microglia within mixed glial cultures for functional experimentation and high-content analysis. *Methods Mol Biol* 2013; **1041**: 41–51.
- 51 Eyupoglu IY, Hahnen E, Heckel A, Siebzehnruhl FA, Buslei R, Fahlbusch R *et al*. Malignant glioma-induced neuronal cell death in an organotypic glioma invasion model. Technical note. *J Neurosurg* 2005; **102**: 738–744.